HOS-BASED MULTI-COMPONENT FREQUENCY ESTIMATION

Maciej Pedzisz, Ali Mansour

Laboratoire "Extraction et Exploitation de l'Information en Environnements Incertains" (E^3I^2)
École Nationale Supérieure des Ingénieurs des Études et Techniques d'Armement (ENSIETA)
2 rue François Verny, 29806 Brest cedex 9, FRANCE
Maciej.Pedzisz{Ali.Mansour}@ensieta.fr
http://www.ensieta.fr/e3i2/

ABSTRACT

We are considering a problem of carrier frequencies recovery for the linear mixtures of two BPSK signals in Gaussian noise. The goal is to simplify further signal analysis: signal separation, modulation identification and parameters estimation. The presented method is based on multidimensional (time-frequency-phase) representation of the Higher Order Statistics (HOS) of the received signal distribution. Performance of the proposed algorithm is verified through extensive simulations and compared to the MUSIC high-resolution spectral estimation method. Corresponding results show that our technique outperforms the latter for all considered frequency shifts, even for high signal-to-noise ratios (SNR).

1. INTRODUCTION

In modern Communication Intelligence (COMINT) systems, there is a need to recognize the applied modulation type [1–6] to more reliably identify the source of an emission or to choose an appropriate method of jamming. All these algorithms assume that received signal is mono-component.

Nowadays, the problem of classifying two or more signals that are closely distributed in a frequency domain is gaining attention. If the signals can't be separated by filtering (or the results are insufficient), the Blind Signal Separation (BSS) approach can be taken into consideration [7–13]. For undetermined problems (less observations than sources), some assumptions have to be made: sources are independent, signal types, characteristic frequencies, as well as timings are known to the receiver.

When these conditions are not met, carrier frequency recovery is enforced at the very beginning. From the COMINT point of view, information concerning the number and types of signals in a mixture is unavailable, limiting the use of some well-known frequency estimation algorithms [14–19].

To overcome these limits and fill the gap between frequency estimation and signal separation/recognition methods, we propose a brand new algorithm based on the constellation rotation of the received signal, and the 2^{nd} and 4^{th} order moments of a 1D distribution of its in-phase component as the functions of frequency and rotation angle. Using the Fourier Series Expansion, we extract noise invariant features which are then used to estimate two frequencies of a linear mixture of two BPSK signals.

2. SIGNAL MODEL

Let us consider a digital modulation scheme with the complex envelope $x(t)$ expressed as:

$$x(t) = \sum_k d_k h(t - kT), \qquad k \in \{1, 2, \ldots, K\} \tag{1}$$

where d_k is a signal's constellation (information contents), $h(t)$ is a pulse shaping function, T is a symbol duration, and K is a number of available symbols.

Taking into account only linear modulations, a multi-component signal $s(t)$ can be expressed as:

$$s(t) = \sum_i A_i x_i(t) \mathrm{e}^{j(\omega_i t + \theta_i)} \tag{2}$$

where A_i, ω_i, and θ_i describe i-th carrier and are accordingly: its amplitude, its frequency and its phase.

Narrowing further analysis by assuming that: $h(t)$ is rectangular, there are two signals in a mixture, and both of them are BPSK types ($d_k \in \{\mathrm{e}^{j0}, \mathrm{e}^{j\pi}\}$)[1], one can express received signal $r(t)$ as:

$$r(t) = A_1 \mathrm{e}^{j(\omega_1 t + \varphi_1(t) + \theta_1)} + A_2 \mathrm{e}^{j(\omega_2 t + \varphi_2(t) + \theta_2)} + n(t) \tag{3}$$

where $\varphi_1(t)$ and $\varphi_2(t)$ are binary sequences:

$$\varphi(t) \in \{0, \pi\}, \quad t \in [kT, (k+1)T[\tag{4}$$

and $n(t)$ is a complex, Additive White Gaussian Noise (AWGN) with probability density functions (PDF) of its real and imaginary parts expressed as:

$$f_{\mathrm{Re[n]}}(n) = f_{\mathrm{Im[n]}}(n) = \mathcal{N}(0, \sigma) \tag{5}$$

with

$$\mathcal{N}(\mu, \sigma) \triangleq \frac{1}{\sigma\sqrt{2\pi}} \exp\left[-\frac{(x-\mu)^2}{2\sigma^2}\right] \tag{6}$$

Without loss of generality, it is assumed that all modulation states $\varphi_k(t)$ are equiprobable i.i.d. processes (independent and identically distributed).

3. ALGORITHM DESCRIPTION

3.1 Theoretical Background

Using the signal model presented in the previous section, one can find a downconverted signal $S(t)$ by means of the complex exponential $\mathrm{e}^{-j(\omega t + \alpha)}$:

$$\begin{aligned} S(t) = {} & A_1 \mathrm{e}^{j((\omega_1 - \omega)t + \varphi_1(t) + \theta_1 - \alpha)} \\ & + A_2 \mathrm{e}^{j((\omega_2 - \omega)t + \varphi_2(t) + \theta_2 - \alpha)} \\ & + n(t) \mathrm{e}^{-j(\omega t + \alpha)} \end{aligned} \tag{7}$$

At every point in time, the PDF of its real part $f_{\mathrm{Re[S]}}(S(t))$ can be expressed by means of 4 gaussian distributions:

$$\begin{aligned} f_{\mathrm{Re[S]}}(S(t)) = {} & \tfrac{1}{4}[\mathcal{N}(s_{11}, \sigma) + \mathcal{N}(s_{12}, \sigma) \\ & + \mathcal{N}(s_{21}, \sigma) + \mathcal{N}(s_{22}, \sigma)] \end{aligned} \tag{8}$$

[1] These assumptions are quite common in the field of BSS.

where mean values s_{kl} correspond to all possible combination of 2 characteristic states (two BPSK signals):

$$\begin{aligned} s_{11} &= A_1\cos((\omega_1-\omega)t-\alpha+\theta_1) \\ &\quad + A_2\cos((\omega_2-\omega)t-\alpha+\theta_2) \end{aligned} \tag{9}$$

$$\begin{aligned} s_{12} &= A_1\cos((\omega_1-\omega)t-\alpha+\theta_1) \\ &\quad + A_2\cos((\omega_2-\omega)t-\alpha+\theta_2+\pi) \end{aligned} \tag{10}$$

$$\begin{aligned} s_{21} &= A_1\cos((\omega_1-\omega)t-\alpha+\theta_1+\pi) \\ &\quad + A_2\cos((\omega_2-\omega)t-\alpha+\theta_2) \end{aligned} \tag{11}$$

$$\begin{aligned} s_{22} &= A_1\cos((\omega_1-\omega)t-\alpha+\theta_1+\pi) \\ &\quad + A_2\cos((\omega_2-\omega)t-\alpha+\theta_2+\pi) \end{aligned} \tag{12}$$

Knowing that distribution (8) is symmetric with respect to the origin, and using the formulas for 2nd and 4th order moments of Gaussian distribution:

$$m_2^g = \mu^2+\sigma^2, \qquad m_4^g = \mu^4+6\mu^2\sigma^2+3\sigma^4 \tag{13}$$

it is straightforward to find moments of $f_{\mathrm{Re[S]}}(S(t))$ as the functions of frequency, phase, and time:

$$\begin{aligned} m_2(\omega,\alpha,t) &= A_1^2\cos((\omega_1-\omega)t-\alpha+\theta_1)^2 \\ &\quad + A_2^2\cos((\omega_2-\omega)t-\alpha+\theta_2)^2+\sigma^2 \end{aligned} \tag{14}$$

$$\begin{aligned} m_4(\omega,\alpha,t) &= A_1^4\cos((\omega_1-\omega)t-\alpha+\theta_1)^4 \\ &\quad + A_2^4\cos((\omega_2-\omega)t-\alpha+\theta_2)^4 \\ &\quad + 6A_1^2\sigma^2\cos((\omega_1-\omega)t-\alpha+\theta_1)^2 \\ &\quad + 6A_2^2\sigma^2\cos((\omega_2-\omega)t-\alpha+\theta_2)^2 \\ &\quad + 6A_1^2A_2^2\cos((\omega_1-\omega)t-\alpha+\theta_1)^2 \\ &\quad \cdot\cos((\omega_2-\omega)t-\alpha+\theta_2)^2+3\sigma^4 \end{aligned} \tag{15}$$

In practice, we have often only one realization of the finite length signal, and what we can observe is the averaged value over the observation period T_0:

$$\overline{m}_2(\omega,\alpha) = \frac{1}{T_0}\int_{-T_0/2}^{+T_0/2} m_2(\omega,\alpha,t)\,dt \tag{16}$$

$$\overline{m}_4(\omega,\alpha) = \frac{1}{T_0}\int_{-T_0/2}^{+T_0/2} m_4(\omega,\alpha,t)\,dt \tag{17}$$

These values can be decomposed into the Fourier Series Expansion as follows:

$$\overline{m}_2(\omega,\alpha) = \tfrac{a_{20}(\omega)}{2} + a_{22}(\omega)\cos(2\alpha) + b_{22}(\omega)\sin(2\alpha) \tag{18}$$

$$\begin{aligned} \overline{m}_4(\omega,\alpha) &= \tfrac{a_{40}(\omega)}{2} + a_{42}(\omega)\cos(2\alpha) + b_{42}(\omega)\sin(2\alpha) \\ &\quad + a_{44}(\omega)\cos(4\alpha) + b_{44}(\omega)\sin(4\alpha) \end{aligned} \tag{19}$$

with

$$a_{kl}(\omega) = \frac{1}{\pi}\int_{-\pi}^{+\pi}\overline{m}_k(\omega,\alpha)\cos(l\alpha)\,d\alpha \tag{20}$$

$$b_{kl}(\omega) = \frac{1}{\pi}\int_{-\pi}^{+\pi}\overline{m}_k(\omega,\alpha)\sin(l\alpha)\,d\alpha \tag{21}$$

In-deep analysis of coefficients $a_{kl}(\omega)$ and $b_{kl}(\omega)$ shows that only combinations $\{kl\}\in\{22,44\}$ provide independence of noise. Additionally, they can be equally represented in terms of amplitude $c_{kl}(\omega)$ and phase $\vartheta_{kl}(\omega)$:

$$c_{kl}(\omega) = \sqrt{a_{kl}^2(\omega)+b_{kl}^2(\omega)} \tag{22}$$

$$\vartheta_{kl}(\omega) = -\arctan\left[\frac{b_{kl}(\omega)}{a_{kl}(\omega)}\right] \tag{23}$$

Neglecting the phase $\vartheta_{kl}(\omega)$, and averaging over all possible initial phases (θ_1,θ_2)

$$C_k(\omega) = \frac{1}{4\pi^2}\int_{-\pi}^{+\pi}\int_{-\pi}^{+\pi} c_{kk}^2(\omega)\,d\theta_1\,d\theta_2 \tag{24}$$

one eventually finds:

$$\begin{aligned} C_2(\omega) &= \frac{A_1^4}{4}\left[\frac{\sin(T_0(\omega-\omega_1))}{T_0(\omega-\omega_1)}\right]^2 \\ &\quad + \frac{A_2^4}{4}\left[\frac{\sin(T_0(\omega-\omega_2))}{T_0(\omega-\omega_2)}\right]^2 \end{aligned} \tag{25}$$

$$\begin{aligned} C_4(\omega) &= \frac{A_1^8}{64}\left[\frac{\sin(2T_0(\omega-\omega_1))}{2T_0(\omega-\omega_1)}\right]^2 \\ &\quad + \frac{A_2^8}{64}\left[\frac{\sin(2T_0(\omega-\omega_2))}{2T_0(\omega-\omega_2)}\right]^2 \\ &\quad + \frac{9A_1^4A_2^4}{16}\left[\frac{\sin(2T_0(\omega-\frac{\omega_1+\omega_2}{2}))}{2T_0(\omega-\frac{\omega_1+\omega_2}{2})}\right]^2 \end{aligned} \tag{26}$$

To visualize these relations we have fixed: $\omega_1=-1$, $\omega_2=1$, and $T_0=4$. Corresponding results for different ratios between amplitudes are presented in the figure 1.

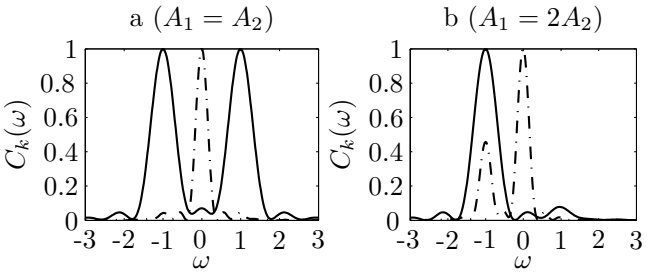

Figure 1: Coefficients $C_2(\omega)$ (solid line) and $C_4(\omega)$ (dash-dot line) for different ratios between amplitudes.

It is clear that by using coefficients $C_2(\omega)$ and $C_4(\omega)$, one can find the following estimators:

$$\widehat{\omega}_{1,2} = \max_{\omega}[C_2(\omega)] \quad \text{(one of two frequencies)} \tag{27}$$

$$\widehat{\omega}_0 = \max_{\omega}[C_4(\omega)] \quad \text{(mean frequency)} \tag{28}$$

Further analysis of the relations between amplitudes in equation (26) shows that estimator $\widehat{\omega}_0$ is valid if

$$\frac{A^8}{64} < \frac{9A^8\eta^4}{16} \Longleftrightarrow \eta > \sqrt{\frac{1}{6}} \approx 0.4 \tag{29}$$

with

$$\eta = \min\left[\frac{A_1}{A_2},\,\frac{A_2}{A_1}\right] \tag{30}$$

To overcome this limit, we propose a modification based on correlations between $C_2(\omega)$ and $C_4(\omega)$. Naming correlations as

$$r_{C_2C_2}(\omega) = C_2(\omega) * C_2(-\omega)^* \tag{31}$$

$$r_{C_2C_4}(\omega) = C_2(\omega) * C_4(-\omega)^* \tag{32}$$

it is possible to prove that function

$$R(\omega) = \frac{r_{C_2C_4}(\omega)}{\max[r_{C_2C_4}(\omega)]} - \frac{r_{C_2C_2}(\omega)}{\max[r_{C_2C_2}(\omega)]} \tag{33}$$

can be used to estimate

$$\max_{\omega}[R(\omega)] \Longleftrightarrow \frac{\widehat{\omega}_1 - \widehat{\omega}_2}{2} \quad \text{or} \quad \frac{\widehat{\omega}_2 - \widehat{\omega}_1}{2} \tag{34}$$

For $A_1 > A_2$, the maximum value of $R(\omega)$ corresponds to $(\widehat{\omega}_1 - \widehat{\omega}_2)/2$; otherwise, to $(\widehat{\omega}_2 - \widehat{\omega}_1)/2$.

Using the same set of parameters as before (as in figure 1), we have visualized the function $R(\omega)$ for different ratios between amplitudes, and the corresponding results are presented in the figure 2.

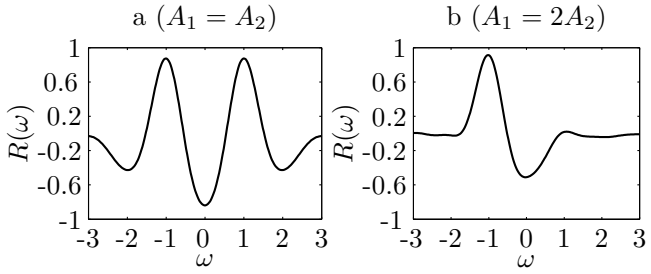

Figure 2: Coefficient $R(\omega)$ for different ratios between amplitudes.

3.2 Practical Implementation

The algorithm can be decomposed into two main parts: a raw estimation, and a fine-tuning part. The aim of the first is to provide a frequency band (Frequency Raster) in which the fine-tuning part will search for exact frequency locations.

First of all, the algorithm estimates power spectral density (PSD) of the received signal by using the Welch [20] modified periodogram method. Next, an heuristic threshold is applied to the PSD to extract only the meaningful part of the signal spectrum. Finally, the extracted part is used to construct a Frequency Raster.

The fine-tuning part is implemented as a downconversion with the frequencies chosen from the Frequency Raster. The resulting baseband signal is then rotated ($\alpha \in [-\pi, \pi]$), and for each α, 2nd and 4th order moments are estimated. Next, the Fourier Series Expansion is applied to extract $C_2(\omega)$ and $C_4(\omega)$. Finally, based on equations (31), (32), and (33), the $R(\omega)$ is computed and the maximum searching algorithm is applied to both $C_2(\omega)$ and $R(\omega)$.

Using the relations (27) and (34), it is simple to find the estimators of two frequencies:

$$\widehat{\omega}_1 = \max_{\omega}[C_2(\omega)] \tag{35}$$

$$\widehat{\omega}_2 = \begin{cases} \omega_{1\_2} & \text{if } C_2(\omega_{1\_2}) > C_2(\omega_{2\_1}) \\ \omega_{2\_1} & \text{otherwise} \end{cases} \tag{36}$$

with

$$\omega_{1\_2} = \widehat{\omega}_1 - 2\max_{\omega}[R(\omega)] \tag{37}$$

$$\omega_{2\_1} = 2\max_{\omega}[R(\omega)] + \widehat{\omega}_1 \tag{38}$$

One must pay attention to the computational complexity of this algorithm. The fact that we do not assume any prior knowledge concerning the locations of the true carrier frequencies makes it necessary to apply the whole Frequency Raster. For every frequency from this raster, we make a downconversion of the entire signal to the baseband, and we rotate resulting constellation using discretized angles. The amount of calculations (complex multiplications) can be important, making this algorithm (in the current state) inapplicable for real-time systems when number of signal samples is large. The methods of reducing the influence on performance of this factor are currently being examined.

4. EXPERIMENTAL RESULTS

To evaluate the performance of the proposed algorithm, extensive simulations were conducted on the linear mixtures of two BPSK signals. Signals were composed of 1025 samples, 5 samples per symbol, 1000 different realizations. The initial phases were randomly chosen from the range $[-\pi, \pi]$, the SNR was varying from 0 dB to 30 dB, and the ratio between amplitudes η was varying from 0.2 to 1. Frequency distance between two signals was fixed to $4/T_0$ ($\approx$ 31 Hz when sampling frequency F_s = 8000 Hz). Corresponding variances[2] are presented in a figures 3.a (estimator $\widehat{\omega}_1$) and 3.b (estimator $\widehat{\omega}_2$) for: $\eta = 0.2$ – solid line, $\eta = 0.6$ – dotted line, and $\eta = 1$ – dashed line.

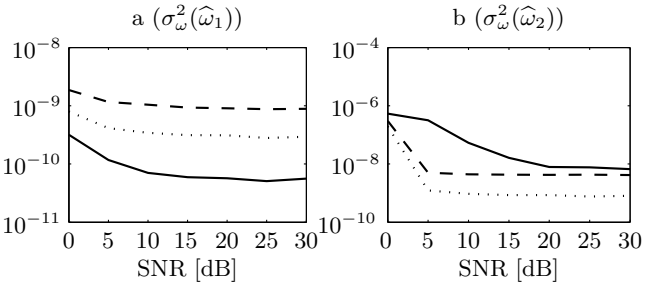

Figure 3: Simulation results for estimators $\widehat{\omega}_1$ and $\widehat{\omega}_2$.

It is clear that best averaged performance of the proposed algorithm is obtained when $\eta \approx 0.5$. For $\eta \to 0$ (only one signal in a mixture), $C_2(\omega)$ has only one dominant maximum (unbiased estimator with variance determined by T_0) which leads to very accurate results for the first frequency, and at the same time, the worst for the second one (there is no second signal). For $\eta \to 1$ (two signals have the same amplitudes), the performance degrades because of the mutual influence between maximals (bias caused by "secondary lobes") for both $C_2(\omega)$ and $R(\omega)$ (*cf.* figures 1.a and 2.a).

The second experiment was conducted to compare our HOS-based Frequency Estimation (HOSFE) technique with a well-known MUSIC [21] spectral estimation method. We have fixed: F_s = 8000 Hz, $\eta = 1$ ($A_1 = A_2$), SNR = 20 dB, 4th order MUSIC method[3], and the shift between two frequencies $\Delta_f T_0 = |f_2 - f_1| T_0$ from 1 to 128 (from $\approx$ 7.82 Hz to $\approx$ 1000 Hz). Corresponding results are presented in the figure 4.a (HOSFE) and 4.b (MUSIC) for estimators: $\widehat{\omega}_1$ – solid lines, and $\widehat{\omega}_2$ – dashed lines.

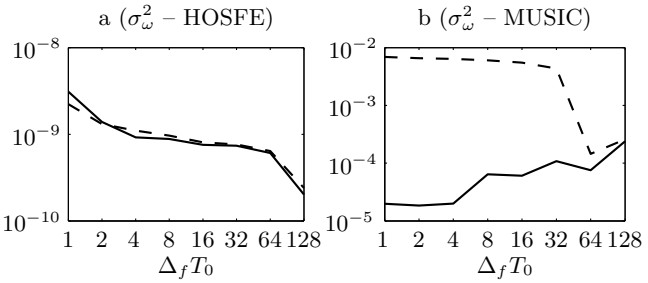

Figure 4: Comparison between HOSFE and MUSIC methods for estimators $\widehat{\omega}_1$ (solid lines) and $\widehat{\omega}_2$ (dashed lines).

There are two advantages of our method compared to the MUSIC method: the variances of both estimators are almost the same, and they decrease when the observation time T_0 and/or

[2] $\sigma^2_\omega(\widehat{\omega}_i) = \mathrm{Var}\{(\widehat{\omega}_i - \omega_i)/2\pi F_s\}$

[3] Simulations for the 2nd and 8th order MUSIC were conducted as well, giving the considerably worse results.

frequency distance Δ_f increases. In the MUSIC case, even if the first frequency is estimated correctly, the second frequency may have a variance which is more than 100 times greater (especially for small frequency shifts). In addition, even for $\Delta_f T_0 > 64$ (variances of both estimators are similar), the performance of our algorithm is almost 10^6 times better compared to the MUSIC method. The averaged variances are: $\sigma_\omega^2 \approx 2.2 \cdot 10^{-10}$ for the HOSFE algorithm, and $\sigma_\omega^2 \approx 2.5 \cdot 10^{-4}$ for the MUSIC method when $\Delta_f T_0 = 128$.

5. CONCLUSION

Our new algorithm is targeted a multi-carrier frequency recovery for linear mixtures of digital, linearly modulated signals in Gaussian noise. The presented method is based on 2^{nd} and 4^{th} order moments of the received signal as the functions of rotation angle and frequency. Extracted features are independent of the initial carrier phases, symbol timings, and are very efficient with respect to SNR. The performance of the algorithm is assessed through extensive simulations and then compared to the MUSIC high-resolution method. Corresponding results show that our technique outperforms the latter for all considered frequency shifts even for high SNR (almost 10^6 times better). Its high accuracy makes it applicable as a preprocessing step for blind signal separation/recognition algorithms.

Although, theoretical background and simulation results are provided only for mixtures of two BPSK signals, extension to more than two BPSK signals in a mixture is straightforward: $C_2(\omega)$ will have as many peaks (of type $\text{Sinc}^2(x)$) as signals, and $R(\omega)$ will contain peaks which correspond to different combination of type $(m\omega_1 \pm n\omega_2)/2$. In this case, the problem appears when $A_1 \neq A_2 \neq A_3 \ldots$ – components with small amplitudes will be hardly visible in $C_2(\omega)$, and one must take into consideration the peaks from $R(\omega)$. For a large number of components, there will be large number of possible combinations between the frequencies, and ambiguous results will determine the overall performance.

An in-depth analysis of this problem, as well as extension of this method for the case with: other than BPSK signal types (ex. QPSK or QAM), convolutive mixtures and more realistic filter types (raised-cosine filter instead of rectangular one), are our current topics of interest.

REFERENCES

[1] E.E. Azzouz, A.K. Nandi, *Automatic Modulation Recognition of Communication Signals*, Kluwer Academic Publishers, 1996.

[2] C.J. Le Martret, *Modulation Classification by Means of Different Order Statistical Moments*, in MILCOM 1997, Monterey, USA, October 1997.

[3] Y. Yang, C.-H. Liu, *An Asymptotic Optimal Algorithm for Modulation Classification*, in IEEE Comm. Lett., vol. 2, no. 5, pp. 117-119, May 1998.

[4] A. Swami, B.M. Sandler, *Hierarchical Digital Modulation Classification Using Cumulants*, in IEEE Trans. on Comm., vol. 48, no. 3, pp. 416-429, March 2000.

[5] O.A. Dobre, Y. Bar-Ness, W. Su, *Higher-Order Cyclic Cumulants for High Order Modulation Classification*, in MILCOM 2003, Boston, USA, October 2003.

[6] M. Pedzisz, A. Mansour, *Automatic Modulation Recognition of MPSK Signals Using Constellation Rotation and its 4-th Order Cumulant*, to be published in Elsevier Digital Signal Processing, 2005.

[7] T.-W. Lee, M.S. Lewicki, M. Girolami, T.J. Sejnowski, *Blind Source Separation of More Sources Than Mixtures Using Overcomplete Representations*, in IEEE Sig. Proc. Let., vol. 6, no. 4, April 1999.

[8] K.I. Diamantaras, *Blind Separation of Multiply Binary Sources using a Single Linear Mixture*, in ICASSP 2000, Istanbul, Turkey, June 2000.

[9] L. Benaroya, F. Bimbot, *Wiener Based Source Separation with HMM/GMM Using a Single Sensor*, in Report GdR ISIS, Paris, France, 12 June 2003.

[10] Y. Li, A. Cichocki, S. Amari, *Sparse Component Analysis for Blind Source Separation with Less Sensors than Sources*, in ICA 2003, Nara, Japan, April 2003.

[11] L. Albera, A. Ferréol, P. Comon, P. Chevalier, *Sixth Order Blind Identification of Undetermined Mixtures (BIRTH) of Sources*, in ICA 2003, Nara, Japan, April 2003.

[12] A. Mansour, M. Kawamoto, C. Puntonet, *A Time-Frequency Approach to Blind Separation of Under-Determined Mixture of Sources*, in IASTED-ASM, Marbella, Spain, 3-5 September 2003.

[13] M. Pedzisz, A. Mansour, *HOS Based Distinctive Features for Preliminary Signal Classification*, in ICA 2004, Granada, Spain, September 2004.

[14] S. Kay, *A Fast and Accurate Single Frequency Estimator*, in IEEE Trans. Acoust. Speech, Sig. Proc., vol. ASSP-37, pp. 1987-1990, December 1989.

[15] M.P. Fitz, *Further Results in the Fast Estimation of a Single Frequency*, in IEEE Trans. on Comm., vol. 42, no. 2/3/4, pp. 862-864, Feb./Mar./Apr. 1994.

[16] M. Luise, R. Reggiannini, *Carrier Frequency Recovery in All-Digital Modems for Burst-Mode Transmissions*, in IEEE Trans. on Comm., vol. 43, no. 2/3/4, pp. 1169-1178, Feb./Mar./Apr. 1995.

[17] B. Dongming, Z. Gengxin, Y. Xinying, *A Maximum Likelihood Based Carrier Frequency Estimation Algorithm*, in World Computer Congress, Beijing, China, 2000.

[18] E. Serpedin, A. Chevreuil, G.B. Giannakis, *Blind Channel and Carrier Frequency Offset Estimation Using Periodic Modulation Precoders*, in IEEE Trans. on Sig. Proc, vol. 48, no. 8, pp. 2389-2404, August 2000.

[19] M. Pedzisz, A. Mansour, *Carrier Synchronization Based on Renyi's Entropy*, in SoftCOM 2004, pp. 498 – 501, Split, Croatia, 10-13 October 2004

[20] P.D. Welch, *The Use of Fast Fourier Transform for the Estimation of Power Spectra: A Method Based on Time Averaging Over Short Modified Periodograms*, in IEEE Trans. on Audio and Electroacoustics, AU-15, pp. 70-73, June 1967.

[21] S.L. Marple, *Digital Spectral Analysis*, Prentice-Hall, 1987